Mon. Not. R. Astron. Soc. **371,** 1351–1358 (2006) doi:10.1111/j.1365-2966.2006.10755.x

White dwarf stars as strange quark matter detectors – III

O. G. Benvenuto★†

Facultad de Ciencias Astronómicas y Geofísicas, Universidad Nacional de La Plata, Paseo del Bosque S/N, B1900FWA, La Plata, Argentina

Accepted 2006 June 28. Received 2006 June 8; in original form 2006 April 10

ABSTRACT

We continue the study of the properties of non-radial pulsations of strange dwarfs. These stars are essentially white dwarfs with a strange quark matter (SQM) core. We have previously shown that the spectrum of oscillations should be formed by several, well-detached clusters of modes inside which the modes are almost evenly spaced. Here, we study the relation between the characteristics of these clusters and the size of the SQM core. We do so assuming that, for a given cluster, the kinetic energy of the modes is constant. For a constant amplitude of the oscillation at the stellar surface, we find that the kinetic energy of the modes is very similar for the cases of models with $\mathrm{Log}Q_{\mathrm{SQM}} = -2$, -3 and -4, while it is somewhat lower for $\mathrm{Log}Q_{\mathrm{SQM}} = -5$ (here $Q_{\mathrm{SQM}} \equiv M_{\mathrm{SQM}}/M$; M_{SQM} and M are the masses of the SQM core and the star, respectively). Remarkably, the shape (amplitude of the modes versus period of oscillation) of the clusters of periods is very similar. However, the number of modes inside each cluster is strongly (and non-monotonously) dependent upon the size of the SQM core.

The characteristics of the spectrum of oscillations of strange dwarf stars are very different from the ones corresponding to normal white dwarfs and should be, in principle, observable. Consequently, the stars usually considered as white dwarfs may indeed provide an interesting and affordable way to detect SQM in an astrophysical environment.

Key words: dense matter – stars: oscillations – white dwarfs.

1 INTRODUCTION

Long ago, it has been proposed (Bodmer 1971; Terazawa 1979; Witten 1984) that a form of quark matter known as strange quark matter (hereafter SQM), which is a particular form of quark matter with a high content of strangeness per baryon $s/n_{\mathrm{B}} \approx -1$, may be the actual ground state of hadronic matter. Since the publication of these seminal papers, several researchers have explored the cosmological and astrophysical consequences of this hypothesis and the observable quantities that may offer decisive signals supporting the actual existence of SQM. For a recent review on SQM, see Weber (2005).

Here, we are interested in the properties of strange dwarf stars (SDs), objects very similar to standard white dwarfs (WDs) that contain a SQM core. The possible existence of these objects has been proposed sometime ago by Glendenning, Kettner & Weber (1995a,b). The main modification of the structure of SDs as compared to WDs is that SDs have strongly compressed, normal matter layers surrounding the SQM core. If we adhere to the simplest description of SQM properties (the well-known MIT bag model; see e.g. Farhi & Jaffe 1984), we can set an absolute upper limit for the size of the SQM core inside SDs, which is imposed by the requirement that normal matter layers must have densities below the 'neutron drip' density ($\rho_{\mathrm{drip}} \approx 4 \times 10^{11}\,\mathrm{g\,cm^{-3}}$). For higher densities, normal matter should spontaneously drip neutrons on to the SQM core. Then, these neutrons are swallowed and converted to SQM. This makes the size of the SQM core and the density of the normal matter to grow, and we arrive to an unstable situation.

The existence of quark matter somewhere in the Universe is one of the fundamental open problems of physics. If some chunks of SQM were free floating in the Universe, some of them should be swallowed by a (previously) normal WD, which now becomes a SD. Of course, this could also happen previously, during the main sequence or pre-WD evolution. From an astrophysical point of view, WDs are regarded as well-studied objects. For example, it is known that some of them are variable, which is of key importance for the detectability of SQM at their interiors. It seems hardly possible to differentiate a SD from a WD if it is non-variable object (see Benvenuto & Althaus 1996a,b).

Recently, in Benvenuto (2005) and Benvenuto (2006) (hereafter Papers I and II, respectively), it has been studied the non-radial pulsation properties of SDs. It has been found that, due to the extreme compression of the layers surrounding the SQM core, there appears a new resonant cavity for g modes. There, the Brunt–Väisälä frequency has a sharp maximum which, in turn, makes the wavelength of the oscillatory modes to be very short, allowing for the existence of a very rich spectrum of oscillations with consecutive modes very

★E-mail: obenvenu@fcaglp.unlp.edu.ar

†Member of the Carrera del Investigador Científico, Comisión de Investigaciones Científicas de la Provincia de Buenos Aires (CIC), Argentina.

close to each other (Paper I). Detailed numerical calculations have shown that modes should have an amplitude large enough for them to be detectable only in clusters of modes well separate each other (Paper II).

The above mentioned analysis was performed considering the solution of the equations of adiabatic, non-radial pulsations, specifically for dipolar modes [corresponding to $\ell = 1$, where ℓ is the harmonic degree corresponding to the spherical harmonic $Y_{\ell,m}(\theta, \phi)$ which describes the angular dependence of the oscillation pattern] which are the kind of modes usually identified in pulsating WDs. As a matter of facts, the conclusion that observable modes should be located in several clusters well separate each other is based on the analysis of the amplitude of the modes near the SQM core. However, in Paper II we have not computed the kinetic energy (hereafter KE) associated with g modes. Usually, the amplitude of the modes is related with the KE necessary to excite them: a mode with low (high) KE should be easily (hardly) excitable to observable amplitudes. It is the purpose of the present paper to carry out such an analysis performing approximate calculations of the KE associated with the modes. In doing so, we will be able to estimate the *width* of each cluster of modes which, in turn, will allow us to envisage the potential of this method for an observational detection of a SQM core inside a SD. This is the goal of the present paper.

The remainder of the paper is organized as follows. In Section 2, we briefly describe the main pulsational properties of SDs. Then, in Section 3 we present the method we will follow in computing the KE of the modes. In Section 4, we describe the asymptotic treatment we employed to compute the KE of the modes at the layers surrounding the SQM core. Then, in Section 5 we present the KE of the modes at the whole stellar interior as a function of the amount of SQM present at the stellar interior. Finally, in Section 6 we present some concluding remarks related to the main results and conclusions of the present paper.

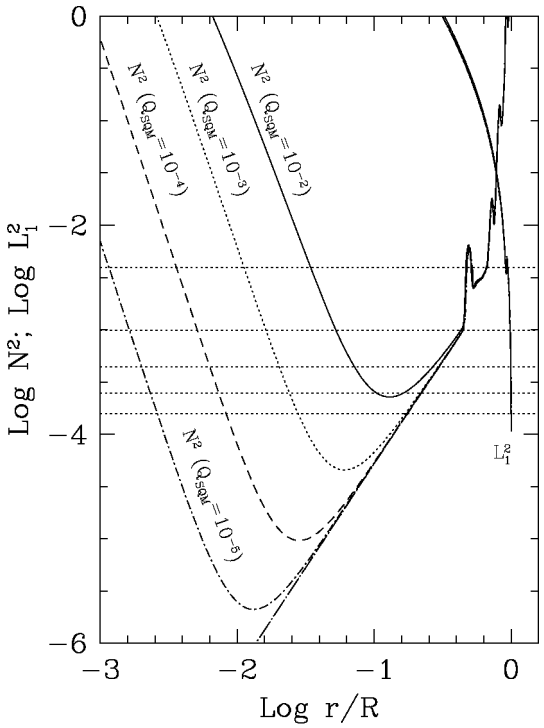

Figure 1. The propagation diagram for SD models of $0.525\,M_\odot$ with $\mathrm{Log}Q_{\mathrm{SQM}} = -2$, -3, -4 and -5 represented with solid, dotted, short dashed and dot–short dashed lines, respectively. Data corresponding to a WD of the same mass and chemical composition are included with dot–long dashed lines. Curves labelled with N^2 depict the square of the Brunt–Väisälä frequency while lines labelled with L_1^2 represent the square of the Lamb frequency for dipolar modes. As a reference, we include with dotted horizontal lines and ordered from above to below, periods for modes with 100, 200, 300, 400 and 500 s. The regions for oscillatory g-modes behaviour are those at which $\sigma < N; L_1$.

2 PROPERTIES OF NON-RADIAL PULSATIONS OF STRANGE DWARF STARS

Here, we will briefly summarize and reanalyse the main results presented in Paper II about the non-radial, adiabatic pulsations of a SD of $0.525\,M_\odot$. We constructed this model starting with a WD model made up of a carbon–oxygen core surrounded by a helium-rich layer and an outermost hydrogen layer (see fig. 1 of Paper II). To that model, we have added SQM cores with fractional mass values of $\mathrm{Log}Q_{\mathrm{SQM}} = -2$, -3, -4 and -5. Q_{SQM} is defined as $Q_{\mathrm{SQM}} \equiv M_{\mathrm{SQM}}/M$, where M_{SQM} and M are the mass of the SQM core and the star, respectively. We have solved the equations of motion for the non-radial, adiabatic pulsations written in terms of dimensionless Dziembowski variables (Unno et al. 1989) subject to adequate boundary conditions at the bottom of the normal fluid phase (see Paper II for details). Note that, for models with effective temperatures T_{eff} in the range at which we observe the variability ($13\,000 \leqslant T_{\mathrm{eff}} \leqslant 11\,000$ K for hydrogen-rich envelope, i.e. DA, WDs) for the cases of $\mathrm{Log}Q_{\mathrm{SQM}} = -2$ and -3, the innermost normal layers are crystallized as consequence of the strong compression induced by the gravitational potential of the SQM core. For the other two (lower) values of Q_{SQM}, normal matter is fluid up to the surface of the SQM core. Due to the enormous compression of the bottom of the normal matter layer, there appears a new resonant cavity for g modes which is a direct consequence of a sharp spike in the Brunt–Väisälä frequency N (see Fig. 1). The regions for oscillatory g-mode behaviour are those at which $\sigma < N; L_\ell$. σ is the angular frequency given by $\sigma = 2\pi/P$ where P is the period of oscillation and L_1 is the Lamb frequency for dipolar modes (see below for definitions).

The resulting spectrum of dipolar oscillations is shown in Fig. 2. Due to the occurrence of the sharp spike in the Brunt–Väisälä frequency, there appears a large number of modes with a period spacing between consecutive modes $\Delta P = P(k) - P(k-1)$ (where k is the number of nodes of a given mode) far lower than the values expected in standard WDs (see the upper panel of Fig. 2). The modes are close enough to each other that it is convenient to represent them with a continuous line. The wavelength of the modes is so short near the SQM core that it has been found quite convenient to treat the modes by means of an asymptotic expansion for $r \leqslant R_{\mathrm{fit}}$, where R_{fit} is the fitting point between asymptotic and numerical treatments. For layers with $X_{\mathrm{fit}} \leqslant x \leqslant 1$, we will perform the standard numerical treatment, where $x = r/R$ and $X_{\mathrm{fit}} = R_{\mathrm{fit}}/R$. In this paper, we assumed $X_{\mathrm{fit}} \approx 0.10$.

The square of the coefficient A [which is proportional to the amplitude of the radial displacement at $x = X_{\mathrm{fit}}$; see equation (33) or also Paper II for derivation] is shown in the bottom panel of Fig. 2. As discussed in Paper II, we expect that the actual, excited modes in SDs should be those with low KE having low amplitude near the compact core, i.e. trapped at the outer layers of the SD. Then, the spectrum of oscillations should be characterized by several, well-detached sets of a large number of modes almost evenly (in period) spaced. Interestingly, we should emphasize that, at least for moderate

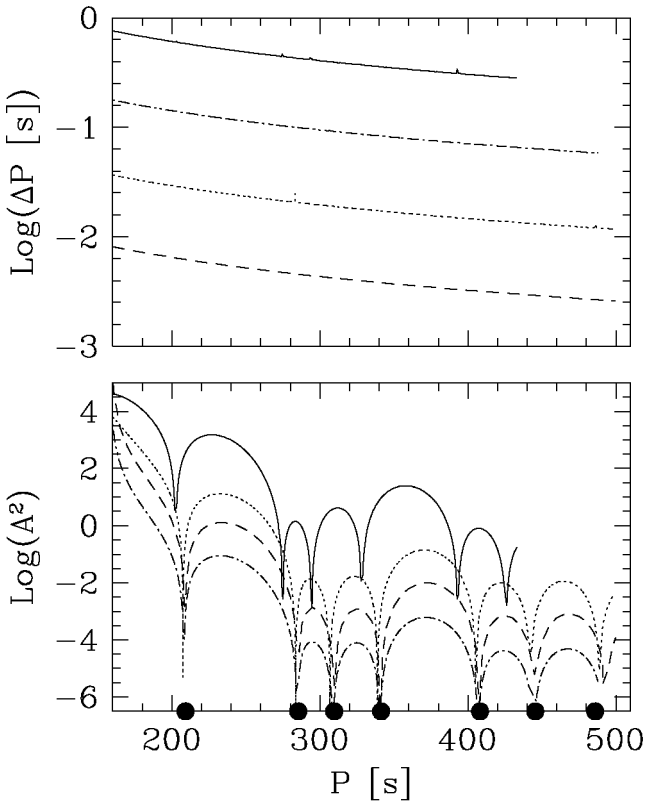

Figure 2. Period spacing of consecutive modes (upper panel) and the coefficient A (proportional to the amplitude of the modes at the layers surrounding the SQM core) of equation (34) (lower panel) as a function of the period of the modes for the cases of $\mathrm{Log}Q_{\mathrm{SQM}} = -2, -3, -4$ and -5 represented with solid, dotted, short dashed and dot–short dashed lines, respectively. On the horizontal axis of the bottom panel, solid circles depict the periods corresponding to dipolar modes of a WD model of the same mass and chemical composition. Note that, at least for the case of moderate sized SQM cores, the minima of the coefficient A (and so, the radial amplitude of the modes) occur very close to these periods values.

values of Q_{SQM}, the minima of the amplitude of the modes near the SQM core occur almost just at the periods at which a standard WD (of the same mass and chemical composition) pulsates. This indicates that one possible signal for the existence of SQM in nature should be to find a fine structure of the spectrum of oscillations at the currently expected pulsation periods for standard WDs. This fine structure should be far richer than what it is expected to be due to rotation, since dipolar modes split in a triplet. Then, no confusion is possible.

We should remark that ΔP is *not* a monotonous function of Q_{SQM}. As a matter of facts, among the considered models, the minimum values of ΔP are found for the case of $Q_{\mathrm{SQM}} = 10^{-4}$. This is due because for this value of Q_{SQM} we found the sharpest peak in the Brunt–Väisälä frequency at non-crystallized layers.

3 KE OF THE MODES

The KE of the modes of oscillation E is given by the integral

$$E = \frac{1}{2}\int_{\mathrm{fluid}} v^2 \mathrm{d}M_{\mathrm{r}}, \tag{1}$$

where v is the velocity of the fluid element and the rest of the symbols have their usual meaning. A more useful expression for E in terms of the radial (ξ_{r}) and horizontal (ξ_{h}) displacements is given by

$$E = 2\pi\sigma^2 \int_{\mathrm{fluid}} \rho\left[\xi_{\mathrm{r}}^2 + \ell(\ell+1)\xi_{\mathrm{h}}^2\right] r^2 \,\mathrm{d}r, \tag{2}$$

which can also be rewritten, in terms of the dimensionless Dziembowski variables y_1 and y_2 as

$$E = 2\pi\omega^2 GMR^3 \int_{\mathrm{fluid}} \left[x^4 y_1^2 + \frac{\ell(\ell+1)}{(C_1\omega^2)^2} x^2 y_2^2\right] \mathrm{d}x. \tag{3}$$

Here,

$$y_1 = \frac{\xi_{\mathrm{r}}}{r}, \quad y_2 = \frac{\sigma^2}{g}\xi_{\mathrm{h}} = \frac{1}{gr}\left(\frac{p'}{\rho} + \Phi'\right), \tag{4}$$

p' and Φ' are the Eulerian (at a fixed coordinate) variations of the equilibrium values of the pressure p and the gravitational potential Φ, respectively. g is the local gravitational acceleration. ω^2 is the dimensionless square of the angular frequency of oscillation given by

$$\omega^2 = \frac{\sigma^2 R^3}{G M}. \tag{5}$$

The dimensionless quantity C_1, inherent to the non-perturbed model, is defined as

$$C_1 = \left(\frac{r}{R}\right)^3 \frac{M}{M_{\mathrm{r}}}. \tag{6}$$

In order to compute the KE of the modes, we have to extend the integration only over the fluid part of the star. Moreover, because of the reasons given above, we will separately treat the compressed layers from those located outside the fitting point. Therefore, we will apply equation (3) for $x \geqslant X_{\mathrm{fit}}$ and define this KE as E_{NA}.

In Fig. 3, we show the KE of the modes corresponding to the layers outside the fitting point E_{NA}. We find that, at the corresponding periods, E_{NA} is very similar to the KE of the modes of a standard

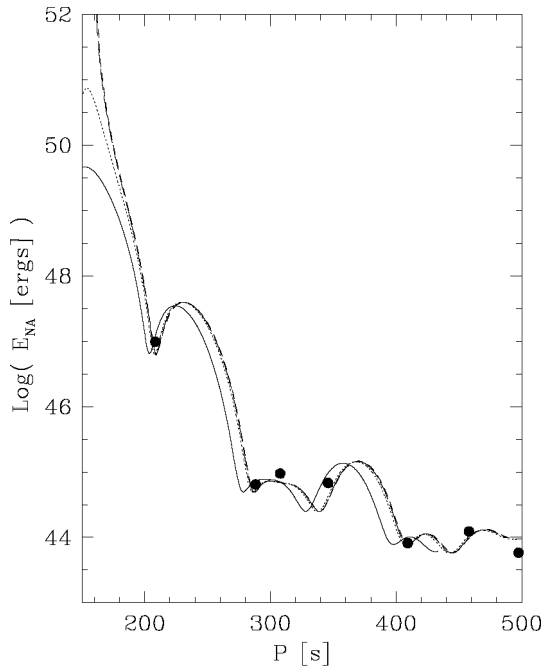

Figure 3. KE of dipolar pulsation modes in the outer part of the SDs ($x \geqslant X_{\mathrm{fit}}$) normalized (as usual) for a radial amplitude equal to the stellar radius. Solid circles depict the KE corresponding to dipolar modes of a WD model of the same mass and chemical composition. Lines are coded as in Fig. 2.

WD of the same mass and chemical composition. Then, in normal WDs, layers with $r \leqslant R_{\rm fit}$ do a minor contribution to the total KE. Consequently, the main differences between the KE of the modes in SDs and WDs will be due to these internal layers. Remarkably, $E_{\rm NA}$ is slightly sensitive to the value of $Q_{\rm SQM}$. As it can be expected, the dependence of the KE of the modes with $Q_{\rm SQM}$ will be dominated by the innermost fluid layers ($r \leqslant R_{\rm fit}$). Now, let us now compute the contribution of the oscillating part of the modes corresponding to the innermost cavity.

4 ASYMPTOTIC TREATMENT NEAR THE COMPACT CORE

The region inside which we will perform an asymptotic treatment ($r \leqslant R_{\rm fit}$) is divided in an inner oscillatory and an outer evanescent zones.[1] The first occurs for $R_{\rm b} \leqslant r \leqslant R_{\rm tp}$ (where $R_{\rm b}$ is the radius at which occurs the bottom of the fluid layer and $R_{\rm tp}$ is the position of the turning point); the second is found at $R_{\rm tp} \leqslant r \leqslant R_{\rm fit}$. In computing the contribution of the asymptotic region to the total KE of the modes, we will calculate the KE due to the truly oscillating region separately from that due to the evanescent one. This is a natural procedure in view of the very different behaviour of any mode in these regions.

Here, we will briefly describe the asymptotic treatment we will employ. We will follow Unno et al. (1989), and assume the Cowling approximation (i.e. we neglect the perturbations of the gravitational potential) which is almost exact in these conditions. In this approximation, we can write the equations of motion as

$$\frac{{\rm d}\alpha}{{\rm d}r} = h(r)\frac{r^2}{c^2}\left(\frac{L_\ell^2}{\sigma^2} - 1\right)\beta, \tag{7}$$

$$\frac{{\rm d}\beta}{{\rm d}r} = \frac{\sigma^2 - N^2}{r^2 h(r)}\alpha. \tag{8}$$

The dependent variables are defined as

$$\alpha \equiv \xi_{\rm r} r^2 \exp\left(-\int_{R_{\rm b}}^{r} \frac{g}{c^2}\,{\rm d}r\right), \tag{9}$$

$$\beta \equiv \sigma \xi_{\rm h} r \exp\left(-\int_{R_{\rm b}}^{r} \frac{N^2}{g}\,{\rm d}r\right) \tag{10}$$

and

$$h(r) = \exp\left[\int_{R_{\rm b}}^{r}\left(\frac{N^2}{g} - \frac{g}{c^2}\right){\rm d}r\right]. \tag{11}$$

In these expressions, c is the velocity of sound; N is the Brunt–Väisälä frequency and L_ℓ is the Lamb frequency given, respectively, by

$$N^2 = g\left(\frac{1}{\Gamma_1}\frac{{\rm d}\ln p}{{\rm d}r} - \frac{{\rm d}\ln \rho}{{\rm d}r}\right) \tag{12}$$

and

$$L_\ell^2 = \ell(\ell+1)\frac{c^2}{r^2}. \tag{13}$$

Γ_1 is the first adiabatic index.

[1] In this paper, we will not consider periods longer than ≈400 s for the case of $Q_{\rm SQM} = 10^{-2}$ because the evanescent zone vanishes (see Fig. 2). Then, the employed inner boundary condition (equation 33; see below) is no longer valid.

Let us replace $\xi_{\rm r}$ and $\xi_{\rm h}$ from equations (9) and (10) in equation (2). A straightforward manipulation leads to the expression

$$E_A = 2\pi\sigma^2 \int_{R_{\rm b}}^{R_{\rm fit}} \rho\left[\exp\int_{R_{\rm b}}^{r}\frac{2g}{c^2}\,{\rm d}r\right] \times\left[\left(\frac{\alpha}{r}\right)^2 + \frac{1}{\ell(\ell+1)}\left(\frac{{\rm d}\alpha}{{\rm d}r}\right)^2\right]{\rm d}r, \tag{14}$$

where E_A is the KE of the layers with $r \leqslant R_{\rm fit}$.

Taking advantage of the fact that at this region of the star, the equation of state of the material approximately corresponds to ultrarelativistic, almost fully degenerate electrons ($P \propto \rho^{4/3}$), we find that $c^2 = (4/3)\,(P/\rho)$. Replacing, we find an expression useful in solving analytically the integral factor in the integrand of equation (14) as follows. Employing the equation of hydrostatic equilibrium, we have

$$\frac{2g}{c^2} = -\frac{3}{2}\frac{{\rm d}\ln P}{{\rm d}r}; \tag{15}$$

then

$$\exp\int_{R_{\rm b}}^{r}\frac{2g}{c^2}\,{\rm d}r = \exp\left(-\frac{3}{2}\int_{R_{\rm b}}^{r}\frac{{\rm d}\ln P}{{\rm d}r}\,{\rm d}r\right) = \left(\frac{P_{R_{\rm b}}}{P}\right)^{3/2} = \left(\frac{\rho_{R_{\rm b}}}{\rho}\right)^2, \tag{16}$$

where $P_{R_{\rm b}}(\rho_{R_{\rm b}})$ is the pressure (density) at the bottom of the fluid part of the star. We find

$$E_A = 2\pi\sigma^2\rho_{R_{\rm b}}^2 \int_{R_{\rm b}}^{R_{\rm fit}} \frac{1}{\rho}\left[\left(\frac{\alpha}{r}\right)^2 + \frac{1}{\ell(\ell+1)}\left(\frac{{\rm d}\alpha}{{\rm d}r}\right)^2\right]{\rm d}r. \tag{17}$$

Now, in order to proceed further, we do need to consider the asymptotic solutions of the equations of motion. Let us consider the change of variables (Unno et al. 1989)

$$\alpha = v\sqrt{\frac{\|P\|}{\rho_{R_{\rm b}}}}, \tag{18}$$

where

$$P = h(r)\frac{r^2}{c^2}\left(\frac{L_\ell^2}{\sigma^2} - 1\right) \approx \frac{\ell(\ell+1)}{\sigma^2}h(r). \tag{19}$$

Then, for $R_{\rm b} \leqslant r \leqslant R_{\rm tp}$, we can write v as

$$v = \frac{1}{\sqrt{\pi k_{\rm r}}}\left[a\cos\left(\int_r^{R_{\rm tp}} k_{\rm r}\,{\rm d}r - \frac{\pi}{4}\right) + b\sin\left(\int_r^{R_{\rm tp}} k_{\rm r}\,{\rm d}r - \frac{\pi}{4}\right)\right], \tag{20}$$

whereas for $R_{\rm tp} \leqslant r \leqslant R_{\rm fit}$

$$v = \frac{1}{\sqrt{\pi\kappa}}\left[\frac{a}{2}\exp\left(-\int_{R_{\rm tp}}^{r}\kappa\,{\rm d}r\right) - b\exp\left(\int_{R_{\rm tp}}^{r}\kappa\,{\rm d}r\right)\right]. \tag{21}$$

In these expressions,

$$k_{\rm r}^2 = \frac{\left(\sigma^2 - L_\ell^2\right)(\sigma^2 - N^2)}{c^2\sigma^2} \tag{22}$$

and $\kappa^2 = -k_{\rm r}^2$.

Considering equation (16), we find

$$\sqrt{\|P\|} = \frac{1}{\sigma}\sqrt{\ell(\ell+1)\frac{\rho}{\rho_{R_\mathrm{b}}}}. \tag{23}$$

Then,

$$E_A = 2\pi\ell(\ell+1)\int_{R_\mathrm{b}}^{R_\mathrm{fit}}\left[\left(\frac{v}{r}\right)^2 + \frac{1}{\ell(\ell+1)}\left(\frac{\mathrm{d}v}{\mathrm{d}r}\right)^2\right]\mathrm{d}r. \tag{24}$$

Now, let us compute the KE contributions of the oscillating and evanescent zones separately. We define E_A^{osc} and E_A^{ev} as the KE of the oscillating and evanescent zones, respectively. Obviously, $E_A = E_A^{\mathrm{ev}} + E_A^{\mathrm{osc}}$.

4.1 The oscillating zone

We begin treating the oscillating zone. In order to simplify the integrations, we will consider that the wavelength of the oscillation is very short compared to the scale of variation of the rest of the relevant quantities. Then, we will consider the approximation $\langle\sin^2 x\rangle = \langle\cos^2 x\rangle = 1/2$ and $\langle\sin x\cos x\rangle = 0$, where $\langle f(x)\rangle$ means the mean value of a given function $f(x)$ over one spatial wave. Then, we have

$$\left(\frac{v}{r}\right)^2 + \frac{1}{\ell(\ell+1)}\left(\frac{\mathrm{d}v}{\mathrm{d}r}\right)^2 \approx \frac{(a^2+b^2)}{2\pi\sqrt{\ell(\ell+1)}\sigma}\frac{N}{r}, \tag{25}$$

where we have employed

$$k_\mathrm{r} = \frac{\sqrt{\ell(\ell+1)}}{\sigma}\frac{N}{r}. \tag{26}$$

Then, the KE in the oscillatory zone is given by

$$E_A^{\mathrm{osc}} = \frac{\sqrt{\ell(\ell+1)}}{\sigma}(a^2+b^2)\int_{R_\mathrm{b}}^{R_\mathrm{tp}}\frac{N}{r}\,\mathrm{d}r. \tag{27}$$

In order to compute this quantity, we need to relate the coefficients a and b with the amplitude A presented in the lower panel of Fig. 2. This is possible after considering the solution of the evanescent part of the mode.

4.2 The evanescent zone

In this zone, we have $\sigma \gg N$ and $\sigma \ll L_\ell$, then we can approximate κ as $\kappa = \sqrt{\ell(\ell+1)}/r$. This allows us to compute the integrals in equation (21) analytically as

$$\exp\left(\int_{R_\mathrm{tp}}^{r}\kappa\,\mathrm{d}r\right) = \Theta^{\sqrt{\ell(\ell+1)}}, \tag{28}$$

where

$$\Theta = \frac{r}{R_\mathrm{tp}} \geqslant 1. \tag{29}$$

Replacing in equation (21), we have

$$v = \frac{1}{[\ell(\ell+1)]^{1/4}}\sqrt{\frac{R_\mathrm{tp}}{\pi}}\left[\frac{a}{2}\,\Theta^{-\sqrt{\ell(\ell+1)}+1/2} - b\,\Theta^{\sqrt{\ell(\ell+1)}+1/2}\right]. \tag{30}$$

Now, equation (30) allows us to write the expression for the KE of the evanescent zone

$$E_A^{\mathrm{ev}} = 2\sqrt{\ell(\ell+1)}\int_{R_\mathrm{tp}}^{R_\mathrm{fit}}\frac{\mathrm{d}r}{R_\mathrm{tp}}\left[C_1\,\frac{a^2}{4}\,\Theta^{-2\sqrt{\ell(\ell+1)}-1} + C_2\,b^2\,\Theta^{2\sqrt{\ell(\ell+1)}-1} - C_3\,ab\,\tfrac{1}{\Theta}\right], \tag{31}$$

where

$$C_1 = 2 + \frac{1-4\sqrt{\ell(\ell+1)}}{4\ell(\ell+1)},$$

$$C_2 = 2 + \frac{1+4\sqrt{\ell(\ell+1)}}{4\ell(\ell+1)},$$

$$C_3 = \frac{1}{4\ell(\ell+1)}.$$

Equation (31) can be solved analytically to give

$$E_A^{\mathrm{ev}} = \frac{C_1 a^2}{4}\left[1-\Theta_\mathrm{fit}^{-2\sqrt{\ell(\ell+1)}}\right] + C_2\,b^2\left[\Theta_\mathrm{fit}^{2\sqrt{\ell(\ell+1)}}-1\right] - 2C_3\sqrt{\ell(\ell+1)}\,ab\,\ln\Theta_\mathrm{fit}, \tag{32}$$

where $\Theta_\mathrm{fit} = R_\mathrm{fit}/R_\mathrm{tp}$.

4.3 Relation between the amplitudes *a*, *b* and *A*

Now, we need to relate the coefficients a and b with the amplitude computed numerically A. In Paper II and in the lower panel of Fig. 2, we employed the expression (hereafter we will set $\ell = 1$)

$$y_1 = A\left(\Theta_\mathrm{fit}^{\sqrt{2}} + \frac{1}{2}\Theta_\mathrm{fit}^{-\sqrt{2}}\tan\Gamma\right) \tag{33}$$

as one of the inner boundary conditions for the numerical calculation of the modes of oscillation in the outer ($r \geqslant R_\mathrm{fit}$) part of the star.[2] Here Γ is given by

$$\Gamma = \frac{\sqrt{2}}{\sigma}\int_{R_\mathrm{b}}^{R_\mathrm{tp}}\frac{N}{r}\,\mathrm{d}r - \frac{\pi}{4}. \tag{34}$$

Also, we have to consider that at R_b the radial displacement must be zero, which gives

$$a = -b\tan\Gamma. \tag{35}$$

Comparing equations (30) and (33), we find

$$b = 2^{-1/4}\sigma\sqrt{\pi\rho_\mathrm{fit}R_\mathrm{fit}^5}\,A. \tag{36}$$

Now, using equations (35) and (36), we are in conditions to compute the values of the KE in the asymptotic zone by employing equations (27) and (31) and then the total KE of the modes as

$$E = E_\mathrm{NA} + E_A^{\mathrm{ev}} + E_A^{\mathrm{osc}}. \tag{37}$$

[2] Here, we should remark the factor (1/2) which corrects equation (23) of Paper II. Equation (24) of that paper should read

$$y_2 = A\frac{\sigma^2 R_\mathrm{fit}}{g}\left(\Theta_\mathrm{fit}^{\sqrt{2}}\tan\Gamma + \frac{1}{2}\Theta_\mathrm{fit}^{-\sqrt{2}}\right).$$

These minor corrections have no effect on the conclusions of that paper.

5 KE OF THE MODES: NUMERICAL RESULTS

The KE of the dipolar modes is shown in Figs 4–7. We find that the total KE is dominated by the behaviour of the modes inside the highly compressed zone with $r \leqslant R_{\rm fit}$. This is so for the whole interval of sizes of SQM cores considered in this paper.

As expected (Paper II), the KE has several sharp minima which are due to the minima of A (shown in Fig. 2) and then, correspond to

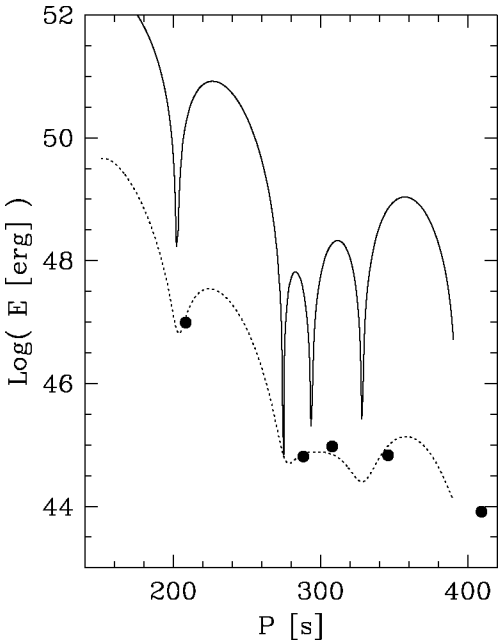

Figure 4. The total KE of the modes for the case of $Q_{\rm SQM} = 10^{-2}$ depicted with a solid line. Dotted line represents the KE of the non-asymptotic layers $E_{\rm NA}$, whereas solid dots stand for the KE corresponding to dipolar modes of a WD model of the same mass and chemical composition. Note that the modes of the WD have KEs comparable to those of $E_{\rm NA}$ for approximately the same period value.

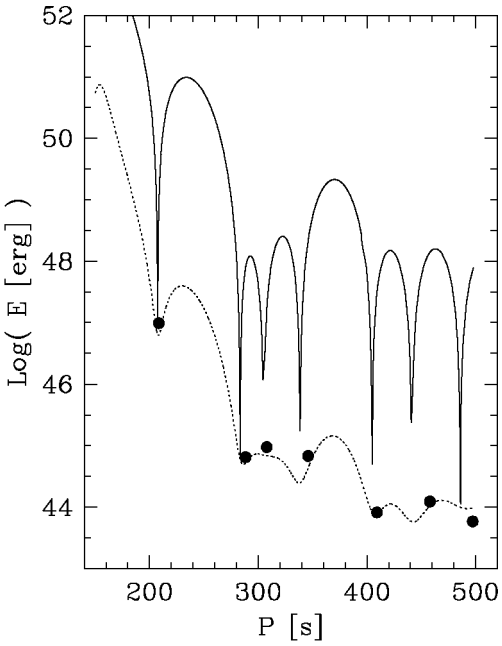

Figure 5. Same as Fig. 4 but for the case of $Q_{\rm SQM} = 10^{-3}$.

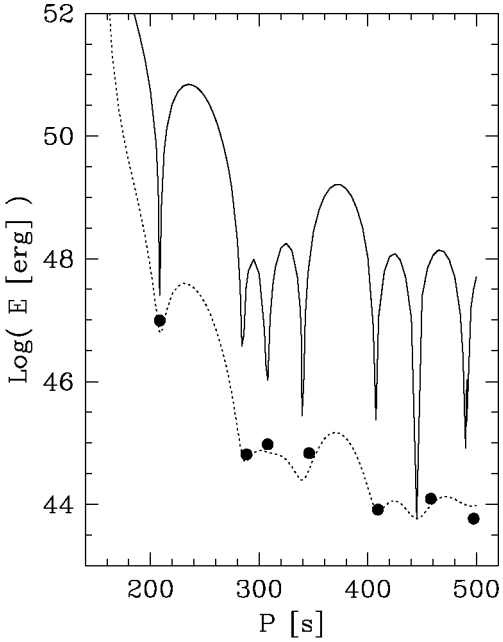

Figure 6. Same as Fig. 4 but for the case of $Q_{\rm SQM} = 10^{-4}$.

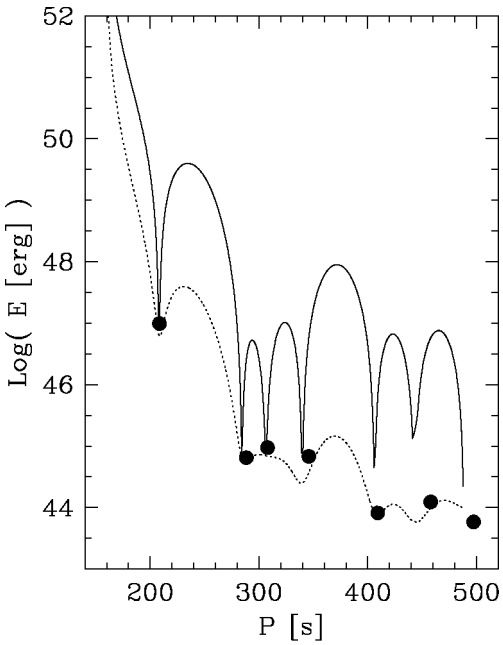

Figure 7. Same as Fig. 4 but for the case of $Q_{\rm SQM} = 10^{-5}$.

period values of very similar to those of the dipolar modes of a WD model of the same mass and chemical composition. Interestingly, the KE of the modes of that WD model is very similar to the values corresponding to the non-asymptotic layers of the SD ($E_{\rm NA}$). The minima in KE corresponds to modes trapped in the layers with $r \geqslant R_{\rm fit}$.

In Fig. 8, we show a comparison between the total KE of the modes for all the considered models. Contrary to what it could be expected, the total KE of the modes shows a dependence with the period of oscillation which is very similar for the cases of $Q_{\rm SQM} = 10^{-2}, 10^{-3}$ and 10^{-4}; meanwhile, for the case of $Q_{\rm SQM} = 10^{-5}$ the

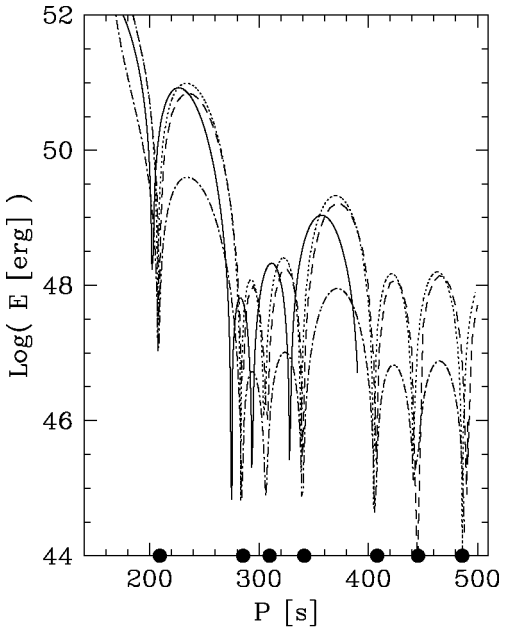

Figure 8. A comparison of the energies for all the models considered in this paper. The meaning of each type of line and solid dots is the same as in Fig. 2.

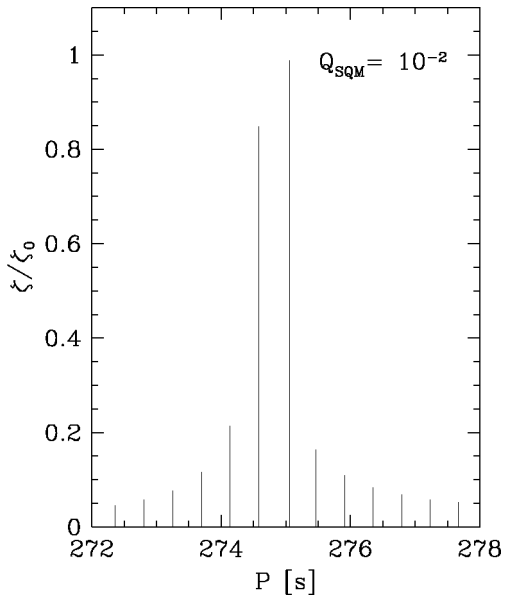

Figure 9. The ratio between the amplitude of the modes and the mode with the maximum amplitude belonging to the cluster of modes centred at $P \approx 275$ s for the case of $Q_{\rm SQM} = 10^{-2}$.

KE is clearly lower. This behaviour is due to two separate reasons. While the amplitude of the oscillation at $R_{\rm fit}$ is a monotonous, increasing function with respect to $Q_{\rm SQM}$ (see lower panel of Fig. 2), the integral in equation (27) has a non-monotonous behaviour. It increases as we change $Q_{\rm SQM} = 10^{-2}$ to 10^{-3}, being even larger for $Q_{\rm SQM} = 10^{-4}$. As stated before, this is due to the fact that for $Q_{\rm SQM} = 10^{-4}$ all normal matter layers are fluid and so, the integral in equation (27) has its maximum value among the here considered models. For the case of models with $Q_{\rm SQM} = 10^{-5}$, not only the amplitude A but also the above mentioned integral have lower values, and so is the KE. In any case, it is remarkable that even with a so small SQM core, the energetics of the modes is governed by the layers surrounding the SQM core. We found that $E_A^{\rm ev} \ll E_A^{\rm osc}$ for all the considered values of $Q_{\rm SQM}$ and modes of oscillation considered in this paper.

Now, we are in a position to study the theoretical predictions regarding the shape of the clusters of modes (amplitude of the modes as a function of the period of oscillation) we expect to find in a variable SD. Here, we will not try to compute the amplitude of the modes considering exciting and damping processes. We will only remark that mode excitation is related to processes occurring in the outermost layers of the star and thus we expect them to operate in a WD or a SD without any essential difference. Here, we will be interested in the shape of each cluster of modes separately. As the modes inside the cluster are very similar to each other (the eigenfunction for $r > R_{\rm fit}$ is almost the same), we expect them to be excited with the *same* KE. While the amplitude at which each cluster of modes is excited will depend on the details of the excitation mechanism and its ability to deposit energy at some particular frequency interval, we do not expect it to be fine-tuned enough to select modes inside each cluster. In other words, we expect that the shape of each cluster of modes will be largely independent of the details of the excitation mechanism.

In the previous figures, we have considered the normalization condition that sets $\xi_{\rm r}(r = R) = R$. Now, let us define ζ as the actual radial amplitude of a mode (i.e. $\xi_{\rm r}(r = R) = \zeta$) belonging to a given cluster. The actual KE of this mode E_* will be given by $E_* = (\zeta/R)^2 E$. If E_* is fixed, we immediately have $\zeta \propto \sqrt{1/E}$. If E_0 and ζ_0 correspond, respectively, to the normalized KE and the actual amplitude of the mode located at the centre of the same cluster of modes, we have

$$\frac{\zeta}{\zeta_0} = \sqrt{\frac{E_0}{E}}. \tag{38}$$

As selected examples of the behaviour found, we show in Fig. 9 the predicted amplitudes of the modes belonging to the cluster of modes centred at 275 s for the cases of $Q_{\rm SQM} = 10^{-2}$. In Fig. 10, we show the corresponding cluster of modes (centred at 283.4 s) for $Q_{\rm SQM} = 10^{-3}$. The results may appear as somewhat paradoxical. The model with the largest considered SQM core ($Q_{\rm SQM} = 10^{-2}$) shows a cluster of modes scarcely populated, while the one with $Q_{\rm SQM} = 10^{-3}$ has a very crowded cluster. In any case, the shape of the clusters is approximately the same.

Some words regarding the observability of such clusters are in order here. We have shown that the width of the predicted clusters is, to some extent, independent of the actual value of $Q_{\rm SQM}$, and is wide enough to be easily observed by means of current studies of pulsating WDs. Note that present asteroseismological observations are precise enough to measure the periods P and even the period derivative $\dot{P}$ of the pulsation modes of some particular objects.[3] In the case of a normal, pulsating WD we expect the Fourier spectrum to be composed of several sharp peaks corresponding to each mode present in the star. In that case, we may expect the peaks to be sharper the longer the time basis of observations is. However, quite contrarily, in the case of the clusters of modes, the peaks should

[3] For the case of the DAV WD G117B15A, the lowest dipolar mode of oscillation is of 215.197 3888 ± 0.000 0004 s (see Kepler et al. 2005). This is a good example of the presently achievable accuracy, far higher than the necessary to reveal the presence of the here predicted clusters of modes.

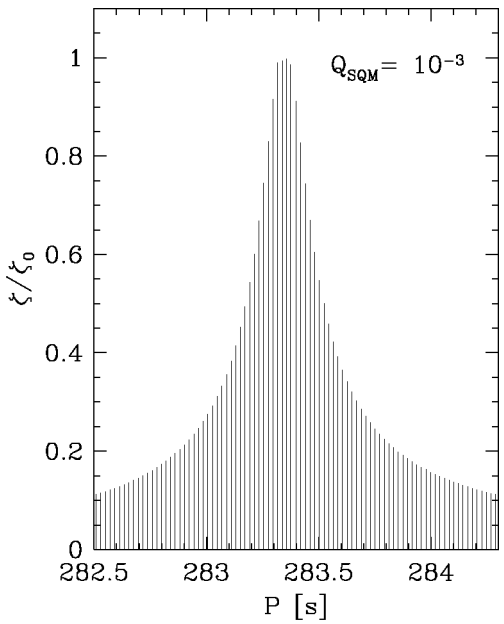

Figure 10. Same as Fig. 9 but for the case of $Q_{\rm SQM} = 10^{-3}$. Note that now the cluster is centred at $P \approx 283.35$ s (this is the closest cluster to $P = 275$ s). This offset is due to the change in the structure of the SD due to the smaller size of the SQM core as compared to the previous figure.

be found to have an *intrinsic* width, clearly distinguishable from the case of a standard WD regardless of the actual value of the parameter $Q_{\rm SQM}$. However, it seems more difficult to resolve the cluster in individual modes in order to measure $Q_{\rm SQM}$. In the case of, e.g., $Q_{\rm SQM} = 10^{-2}$ and 10^{-5} we expect it to be possible without a major difficulty. However, for the intermediate cases considered here, $Q_{\rm SQM} = 10^{-3}$ and 10^{-4}, a long time basis of observations will be necessary (see Paper II for a quantitative discussion of this point).

6 CONCLUDING REMARKS

In this paper, the third of a series, we have investigated the properties of the spectrum of non-radial oscillations of SDs, i.e. objects very similar to standard WDs that contain a SQM core. Here, we have computed the KE necessary to excite dipolar modes to a predetermined amplitude.

We have confirmed the main result of Paper II of this series: we should expect clusters of modes, well detached each other. As a matter of facts, we found that the KE necessary to excite dipolar modes is rather similar for models with $\mathrm{Log}Q_{\rm SQM} = -2$, -3 and -4 while it is somewhat lower for the case of, and $\mathrm{Log}Q_{\rm SQM} = -5$ (where $Q_{\rm SQM} \equiv M_{\rm SQM}/M$). Then, the amplitude of the modes inside each cluster should be very similar. However, the number of modes inside each cluster will be strongly (and non-monotonously) dependent upon the size of the SQM core. Ordering the here considered models with a decreasing number of modes inside each cluster we find the sequence $\mathrm{Log}Q_{\rm SQM} = -4$, -3, -5 and -2. Notably, this is non-monotonous.

These results show, in our opinion, that the study of the oscillation patterns of the currently considered WDs may be of relevance in finding signals for the presence of SQM at their interiors, something that seems to be very difficult by other ways. Moreover, it could be even possible to measure the amount of SQM inside a particular SD by asteroseismological observations. In any case, because of the non-monotonous dependence of the number of modes with $Q_{\rm SQM}$ inside each cluster, for a given object we expect the existence of two solution values for $Q_{\rm SQM}$.

ACKNOWLEDGMENTS

OGB warmly acknowledges Prof. Héctor Vucetich for enlightening discussions about the topic of this work. He also thanks the referee, Prof. Philip Podsiadlowski for his report that has been very useful in improving the original version of the present work.

REFERENCES

Benvenuto O. G., 2005, J. Phys. G, 31, L13 (Paper I)
Benvenuto O. G., 2006, MNRAS, 368, 553 (Paper II)
Benvenuto O. G., Althaus L. G., 1996a, ApJ, 462, 364
Benvenuto O. G., Althaus L. G., 1996b, Phys. Rev. D, 53, 635
Bodmer A. R., 1971, Phys. Rev. D, 4, 1601
Farhi E., Jaffe R. L., 1984, Phys. Rev. D, 30, 2379
Glendenning N. K., Kettner C., Weber F., 1995a, Phys. Rev. Lett., 74, 3519
Glendenning N. K., Kettner C., Weber F., 1995b, ApJ, 450, 253
Kepler S. O. et al., 2005, ApJ, 634, 1311
Terazawa H., 1979, INS-Report-338 (INS, Univ. Tokyo)
Unno W., Osaki Y., Ando H., Saio H., Shibahashi H., 1989, Nonradial Oscillations of Stars, 2nd edn. Univ. Tokyo Press, Tokyo
Weber F., 2005, Prog. Part. Nucl. Phys., 54, 193
Witten E., 1984, Phys. Rev. D, 30, 272

This paper has been typeset from a TEX/LATEX file prepared by the author.